INTERNATIONAL JOURNAL OF MARITIME TECHNOLOGY
IJMT Vol.5/ Winter2016 (41-54)

Available online at: http://ijmt.ir/browse.php?a_code=A-10-450-3&sid=1&slc_lang=en

Technical Notes on the Near Surface Experiments of Submerged Submarine

Mohammad Moonesun[1,2*], Firouz Ghasemzadeh[3],Yuri Korol[4],ValeriNikrasov[4], Alexi Yastreba[1], AlexanderUrsolov[1], Asghar Mahdian[2]

[1*]*National University of Shipbuilding Admiral Makarov (NUOS), PhD candidate ,Ukraine*
[2]*MUT, Department of Marine Engineering,Shahinshahr, Iran;m.moonesun@gmail.com*
[3]Tehran University, *Department of Irrigation and Reclamation Engineering, PhD candidate, Tehran, Iran*
[4]*National University of Shipbuilding Admiral Makarov (NUOS), Department of Hydrodynamics, Professor, Ukraine*

ARTICLE INFO

Article History:
Received: 25 Feb. 2016
Accepted: 15 Mar. 2016

Keywords:
Submarine
Resistance
Experimental
CFD
Snorkel depth
Flow-Vision
Flow-3D

ABSTRACT

In this study, the experimental analysis on the bare hull resistance coefficient of submarine at snorkel depth is represented. The experiments are conducted in marine laboratory of Admiral Makarov University. The results are presented for surface condition and snorkel condition. Snorkel depth is regarded equal to one diameter of submarine hull beneath the water surface as usual in submarines. Performing the experiment at the surface condition is a usual practice process but performing the experiment at submerged condition has several technical notes which are evaluated in this paper. One of challenging discussions is estimating the induced resistance between the main hull and struts. For this part of study, CFD method is used. CFD analyses are conducted by Flow-3D (V.10) software based on solving the RANS equations and VOF method. All analyses are performed for still water condition. The results of this research can be used for AUVs, research submersibles and submarines, torpedoes and every submersible who operate near the free surface of water.

1-Introduction

Submarines have two modes of navigation: surfaced mode and submerged mode. Conventional naval submarines are periodically obliged to transit near the surface of water for surveillance and recovery affairs such as: intake fresh air, charge the high pressure air capsules and start the diesel-generators for recharging the batteries. The process of charging the battery is the most time-consuming task at near surface depth or snorkel depth for usually 6~10 hours that depends on the specifications of electric power system and battery storage. Submarines have usually 220~440 battery cell that should be charged in the period of snorkeling. Minimizing the resistance of a submarine, transiting close to the ocean surface, is very important, because a submarine must save the energy for earlier charging the batteries and lesser need to stay at snorkel depth. If the submarine, waste a lot of energy for propulsion, it needs to stay more and more in snorkel depth. It is a very dangerous situation for a submarine because of the increase in the probability of detection. Common relative dimensions of sailing and mast, and depth in snorkel condition for real naval submarines are shown in Fig.1.

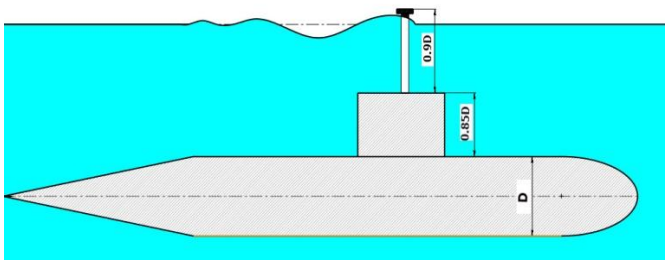

Figure 1. Snorkel depth in naval submarines

Some torpedoes are obliged to approach the free surface too. It depends on the operational demands and the type of torpedo, for example, cruising just beneath the sea surface for receiving the target information by radio electronic devices or satellite. In this condition, the submergence depth of torpedo should be less than 2-3 meters equal to maximum permeability depth of electro-magnetic wave into the water. For every submersible, the more resistance is equal to the more power requirement and thus, lesser range and lesser duration of operation or endurance. In contrast to a surface vessel, a deeply submerged submarine, doesn't encounter the penalty of wave making resistance. Wave making resistance, in critical

Froude numbers, can make up more than 50% of total resistance. When a submarine ascents from the deep depth to the near the surface of water, the free surface effects, causes a steep increase in the resistance because of appearance of wave making resistance. Hydrodynamic aspect in submarine design is discussed by P.N.Joubert [1,2], R.Burcher and L.J.Rydill [3], Y.N.Kormilitsin and O.A.Khalizev[4], U.Gabler[5], L.Greiner[6] and in Ref.[7] by a group of authorities. In surfaced mode of navigation, such as ships, the body interferes with free surface of water. In surface mode in calm water, the wave making resistance is a main part of resistance that depends on the Froude number. For a submarine at the deep depth of the water, there is not wave resistance because there is not a free surface. This depth is named "fully submerged depth". In every depth between surface mode and fully submerged mode, the movement of a submarine or torpedo, causes turbulence on the surface of water. This effect decreases by increasing the depth of submergence but there is a certain depth, which free surface effect and wave resistance is very little and ignorable. In all depths more than this depth, there is fully submerged condition. This paper tries to define this "fully submerged depth". This depth is depended on the dimensions of a submarine. The fully submerged depth, in Refs.[8,9], is defined as a multiple of the outer diameter of submarine hull (D) but in Ref.[10], is defined as a multiple of the length of the submarine hull (L). Fully submerged condition in reference [10] is defined as half of submarine length (h=L/2) and in reference [8] is defined as 3D (h=3D) and in reference [9], this depth is suggested 5D (h=5D). In Refs.[11,12], M.Moonesun et al showed that, according to experimental tests in towing tank for short values of L/D for submarines, the depth, h=5D can be a good suggestion but this depth can be lesser. Now, this paper has concentrated the studies, to find out this depth for high values of L/D and short values of L/D, by CFD method. There are few published scientific articles about the hydrodynamic effects on a submerged body near a free surface, such as dynamics and maneuvering effects by K.Rhee, J.Choi, S.Lee [13], C.Polish, D.Ranmuthugala, J.Duffy, M.Renilson [14] and D.Neulist [15]. Resistance and wave making effects near the free surface are studied by E.Dawson, B.Anderson, S.V.Steel, M.Renilson, D.Ranmuthugala [16], S.Wilson-Haffenden [17] and S.V.Steel [18] which all of them conducted by Australian Maritime Collage. For investigating the wave making resistance of a submarine below the free surface, before this paper, Refs.[17,18] have been the main published articles which both are based on the DARPA SUBOFF submarine model in low Froude numbers. For these analyses, the base method is Experimental Fluid Dynamics (EFD) but to some extent, is reviewed by Computational Fluid Dynamics (CFD). This article wants to extend the studies about resistance of submersibles which travel near the free surface of calm water.Figure 2 shows the resistance coefficient (C_D) which decreases by increasing submergence depth because of increase in the depth, the wave making resistance, decreases.

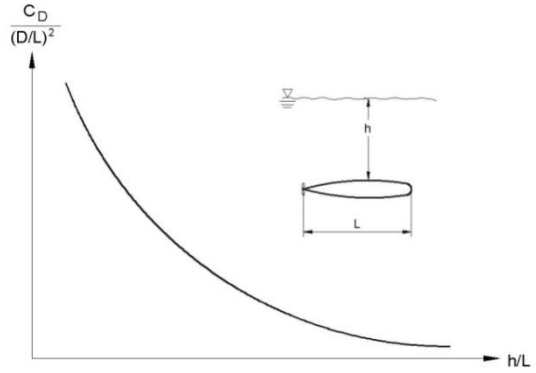

Figure 2: General variations of total Resistance coefficient versus submergence depth

The variations of total resistance versus depth by CFD method (Flow Vision) has studied by Moonesun et.al [19,20] and Behzad [21]. This study has shown a steep decrease in resistance coefficient in depth equal to D and fully submerged depth equal to 4.5D (Fig.3).

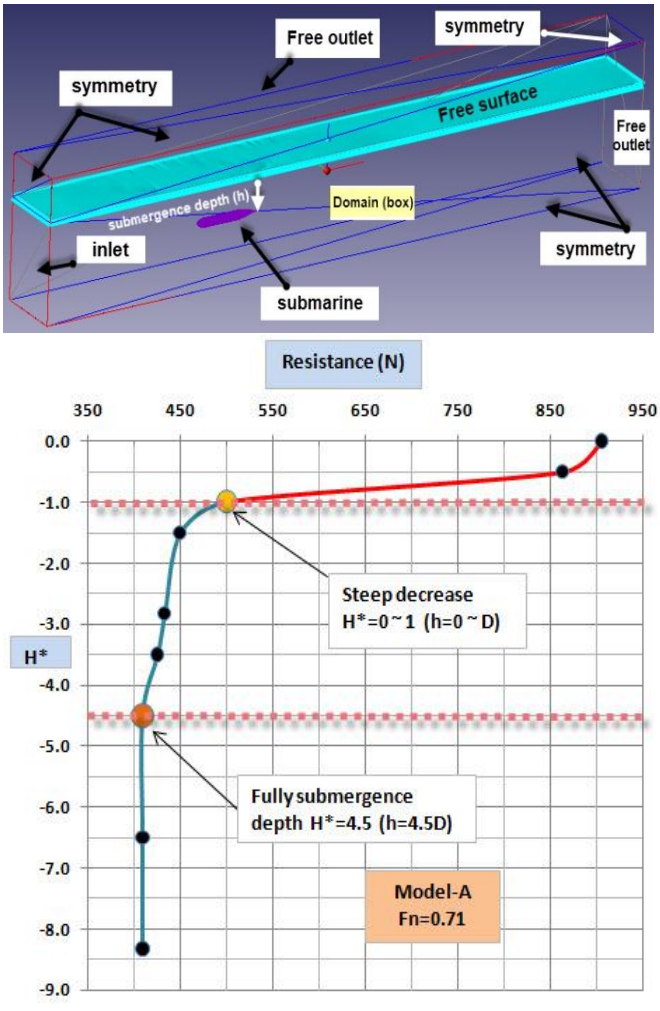

Figure 3. Variations of total resistance versus depth in (modeling in Flow Vision)[19]

An extended experimental studies in this field has been presented in [22]. Some practical notes about the extending the results of submerged model test in towing tank to the full scale submarine is presented in [23]. This paper tries to complete this notes. For conducting the underwater or near surface tests the usual Froude number should be considered. Some technical aspects for conducting the underwater test in towing tank is presented in [24]. According to the Table 1, the usual range of Froude number is 0.2-0.24.

Table 1. Froude number of submarines

Submarine class	Length (m)	Surface speed (knot)	Fn (surface)
TRIOMPHAN	**138**	**20**	**0.28**
DELTA	**167**	**14**	**0.18**
TYPHOON	**172**	**12**	**0.15**
OSCAR II	**144**	**16**	**0.22**
COLLINS	**78**	**10**	**0.19**
DOLPHIN	**57**	**11**	**0.24**
GOTLAND	**67**	**11**	**0.22**
KILO	**73**	**10**	**0.19**
TUPI	**67**	**10**	**0.20**
VICTORIA	**70**	**12**	**0.24**
AKULA	**110**	**10**	**0.16**
U206	**49**	**10**	**0.23**
U209	**64**	**11.5**	**0.24**
Fateh	**45**	**11**	**0.27**

2-Specifications of Model and Towing Tank

2-1- Model

In this study a torpedo shaped submersible (Persia110) is considered. The general form and dimensions of this model is shown in Fig.4. This model is fixed and don't has DOF. This model is the same in CFD method and experiments in towing tank. The model has a volume of 8.38 liters, total area of 0.36 m^2, wetted area in surface draft of 0.26 $m^2$and weight of 8.38 kg. Surface draft is equal to 80mm from beneath the hull and 20mm freeboard. The ratio of L/D is 13 which is inside the range of usual L/D of large naval submarines.

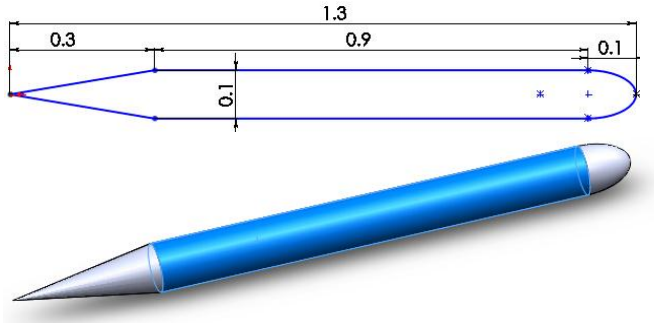

Figure 4. General configuration of the model dimensions of Persia-110 [in meter]

The material density of the model should be near the density of water for earning the natural buoyancy in submerged condition. Fiberglass and wood could not be a good selection because of imposing a stiff positive buoyancy on the dynamometer. Kapraloncould be a good suggestion because of: 1) density of 1.01~1.15. For adjusting the density to the water density, the internal part of the model could be carved according to Fig.5. 2) water tight material 3)easy carving properties. 4) cylindrical traditional form which is similar to the body shape of submarine (Fig.5) and 5)smooth surface.

(a) Traditional cylindrical form of Kapralon

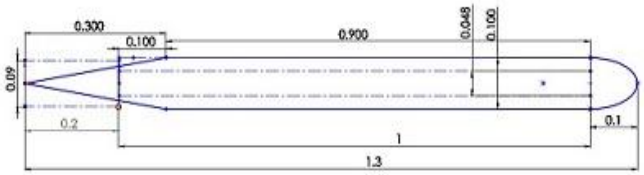

(b) Carving the interior part of Persia-110

Figure 5. Kapralon material for body construction

For conducting the test, two general conditions are considered: 1) surface draft of 90mm. 2) near surface: depth of 100mm from water level to the top of body (equal to depth of strut). Froude numbers are considered according to Tab.2. As mentioned above, the usual range of Froude number of submarines are between 0.2 to 0.24 but here, a wider range is studied. In submerged test, the extracted values more than 1 m/s have encountered a problem because of the sever vibrations in high speeds in struts. Therefore the diagrams of underwater test are represented for values less than 1 m/s.

Table 2. Considered conditions for analyses in two drafts: surface draft and near surface

	V(m/s)	Fn
1	0.196	0.05
2	0.296	0.08
3	0.393	0.11
4	0.492	0.14
5	0.604	0.17
6	0.705	0.20
7	0.803	0.22
8	0.899	0.25
9	0.996	0.28
10	1.397	0.39
11	1.598	0.45
12	1.801	0.50

2-2- The Strut

The cross section of strut is a foil shape as shown in Fig.6-a. Distance between struts is 0.5 meter. More studies have shown that this foil section could not be a good design because of resistance and vibrations. The reason is the existence of free surface effects and the role of wave making resistance. In wind tunnel, because of absence of free surface, symmetric NACA00 foil sections usually are used. Two struts with foil shape form impose about 45% of total resistance. Inversed foil shape struts imposes about 35% resistance. Figure 6-b shows a recommended shape of cross section of strut similar to water plane of ships which two strut of them, impose approximately 25% of total resistance. If a one strut arrangement could be used, it would have a resistance less than 20%. Therefore, the foil section such as Fig.6-a can be the worst selection which should be avoided. A reasonable believe able range of resistance of struts could be about 30% of total resistance.

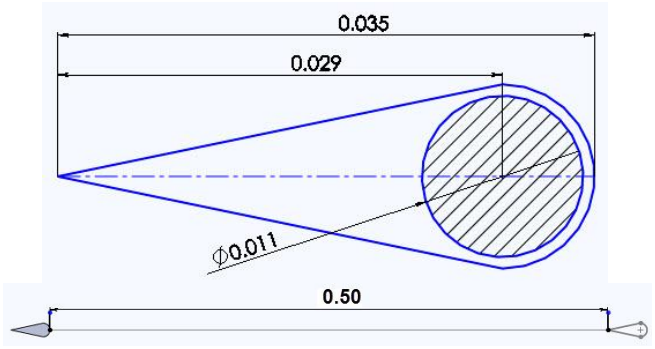

(a) Struts of Persia-110

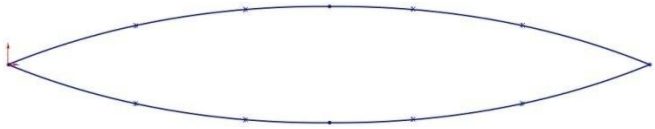

(b) Recommended foil section of strut

Figure 6: Cross section of struts

2-3- Towing Tank

Experimental tests have been performed on the model Persia-110 in the towing tank of Admiral Makarov University, which has 33(m) length, 2.5 (m) width and 1.3 (m) draft (Fig.7). The basin is equipped with a trolley that able to operate in 0.05-6 m/s speed with ±0.02 m/s accuracy. A three degree of freedom dynamometer is used for force and moment measurements. The dynamometer was calibrated by calibration weights and several case studies. The model is fixed without any DOF. The test is in still water and water inside the tank is fresh water.

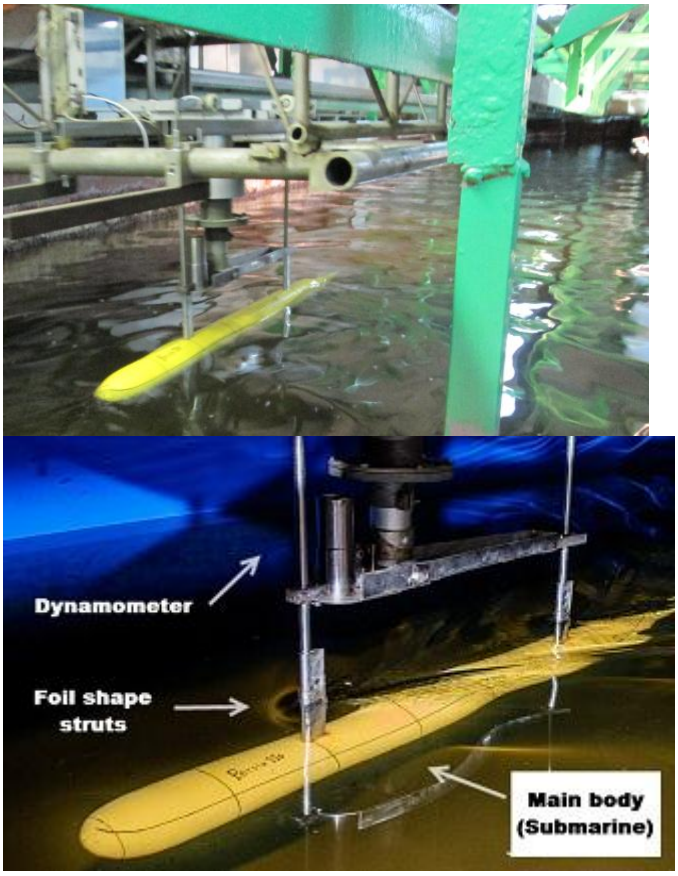

(a) Marine laboratory of Admiral Makarov University

(b) Model Persia-110 according to specifications of Fig.2

Figure 7. Towing tank and model Persia-110

3-Experimental results

3-1- At surface draft

The experimental results at surface draft are presented in Fig.8. It shows a range of 0.012~0.016 for resistance coefficient in common Froude numbers at surface draft. All values of resistance coefficients in this paper are based on wetted area.

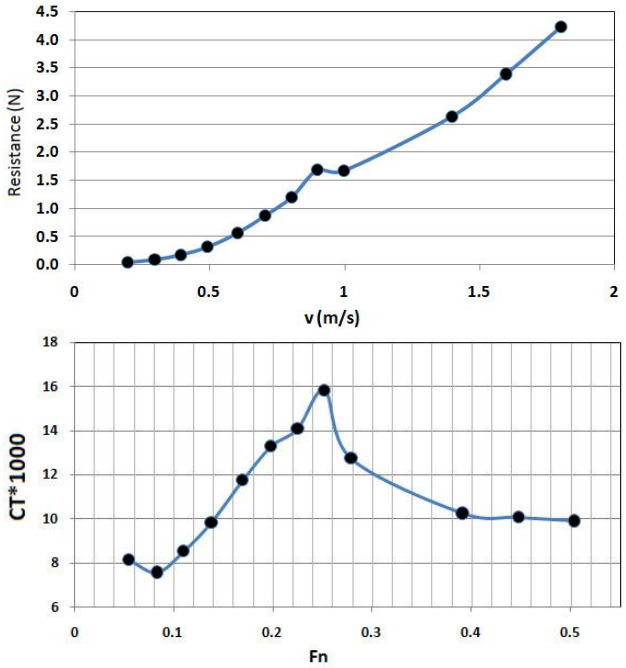

Figure 8. Resistance and resistance coefficient of persia-110 at surface draft

3-2- At snorkel draft

Estimating the resistance of the bare hull of submarine at snorkel depth (100mm) is to some extent more difficult than the surface draft. For extracting the submarine resistance, in first stage, submarine with struts are tested. In second stage, only the struts are tested. The results are shown in Tab.3. At first glance it seems that submarine resistance could be achieved from subtraction of second and third columns of Table 3 but it can't be a right estimation. It is because of the existence of induced resistance of tips of struts. For estimating this induced resistance we have to use CFD method (as mentions in section 4).

Table 3. Resistance in depth of 100mm

V (m/s)	Sub & Struts (N)	Struts (N)
0.196	0.09	0.03
0.296	0.19	0.06
0.393	0.32	0.10
0.492	0.48	0.19
0.604	0.69	0.25
0.705	0.91	0.31
0.803	1.17	0.41
0.899	1.47	0.53
0.996	1.87	0.69

4- Estimation of induced resistance by CFD method

In this section the focus is on the estimation of induced resistance of struts.

4-1- CFD Method of Study

In this research, the dynamic pressure fluctuation has been investigated by a commercially available CFD solver, Flow-3D, developedby Flow ScienceInc.

4-2- Governing Equations

To solve the governing equations of fluid flow, Flow-3Duses a modification of the commonly used Reynolds-average Navier-Stokes (RANS) equations. As the main body of this paper is based on the experimental method, the descriptions of CFD method of study is stated in Appendix-A.

4-3- Conditions of Modeling

The modeling is done in one depth of 100mm from top of the body to the water level. The considered speeds are exactly according to the model test speed. The nine speeds are (m/s): 0.196, 0.296, 0.393, 0.492, 0.604, 0.705, 0.803, 0.899 and 0.996.In every speed three main parts are modeled: 1)submarine and struts 2)only submarine 3)only struts (Figure 9):

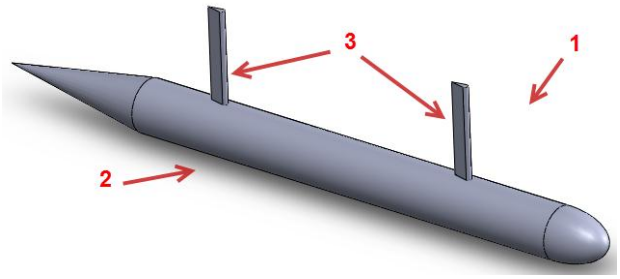

Figure 9. Three main conditions of Modeling

4-4- Domain and Boundary Conditions

The general configurations and dimensions of domain are shown in Fig.10. The length and width are 6.5 and 2.6 meters. Depth is 1.6 meters (1.3meters draft). There boundary conditions are: Input: specified velocity, Output: Specified pressure and other sides are symmetry. The model is situated in depths of 100mm according to Fig.10.a,b. There are three mesh block: one block for the total domain with coarse meshes and other two blocks for fine meshes around the struts and object body. The accuracy of the modeled shape of the struts and body depends on the fine meshes because of small dimensions of struts (Fig.10.c,d). The other settings of CFD modeling are presented in Table 4.

Table 4. Settings of CFD simulation

Elements	Boundary conditions	Descriptions	
Domain	Cubic	conditions	with free surface - domain with inlet, outlet and symmetry - without heat transfer- with current velocity equal to considered submarine speed
		dimensions	L*B*D=6.5*2.6*1.6 m- draft 1.3 m
		grid	structured grid- hexahedral cells-without skew- three mesh block- more fine meshes in mesh block 3 around the struts and main body- Mesh numbers: 1000.000 in mesh block1, 1000.000 in mesh block2, 500.000 in mesh block3, aspect ratio 1 in each block, expansion factor 1 in each block, expansion factor between blocks less than 2.
		settings	Simulation time: 10 sec- Time step=0.0003-0.0005 sec
Fluid	-	Incompressible fluid (fresh water)- tempreture:20 deg- ρ=999.841 kg/m^3- turbulent modeling: Standard k-ε	
Object	GMO	Submarine, length:1.3m, Diameter:0.1, DOF =0	
Boundaries	Inlet	Specified velocity (different for each submarine speed), mean fluid depth 1.3 m	
	Outlet	Specified pressure (Specified fluid level: 1.3 m)	
	Symmetry	In 4 faces	
Initial conditions		Fluid level: 1.3 m, velocity (m/s): equals to specified velocity in Inlet	

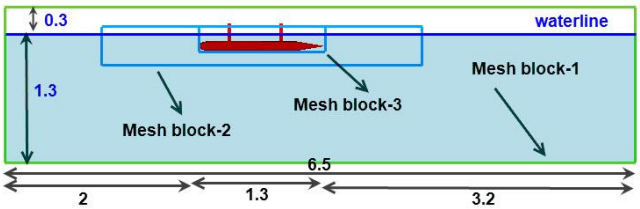

(a) Dimensions of Domain (in meter)

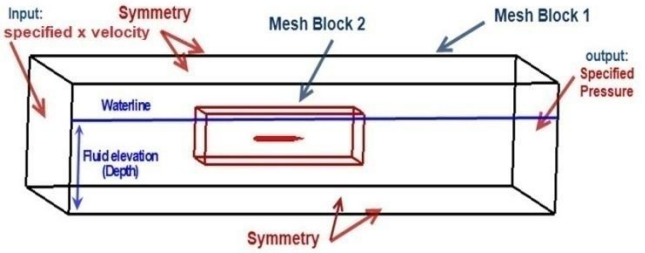

(b) Boundary conditions in domain

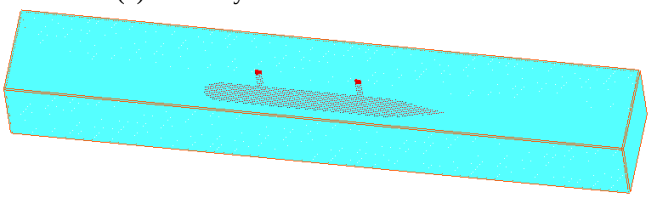

(c) Fine meshes in Mesh Block2

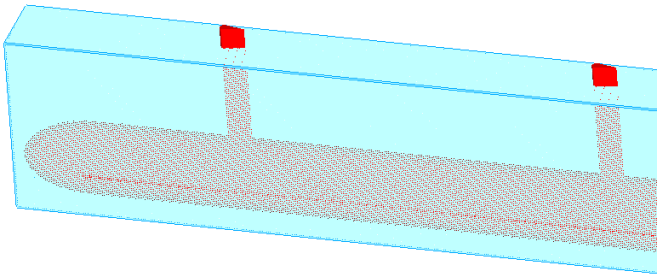

(d) Very fine meshes in Mesh Block 3

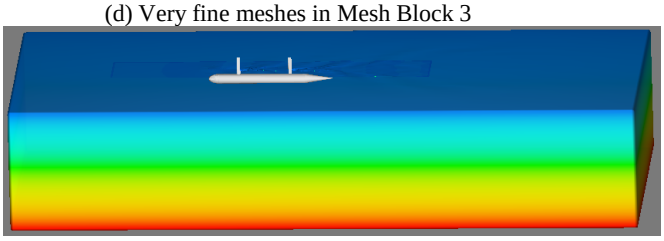

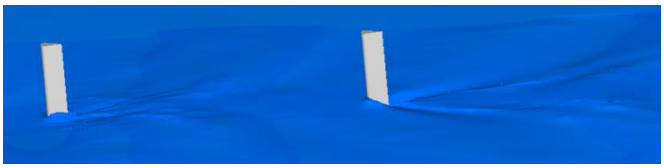

(e) Free surface modeling

Figure 10. Domain and Boundary Conditions in Flow-3D

4-5- Validation and Verification

For validating the results of Flow-3D modeling, one of the results of experimental tests has been considered on the model Persia-110 (Fig.11).

The experiment was performed in surface condition at the draft of 8 cm and speed of 1 m/s. The CFD modeling (Fig.11) was adjusted exactly according to the experimental conditions. Comparison of Fig 11-a and Fig 11-b shows a good agreement between experimental and CFD results. The form of free surface has a good compatibility. The resistance of the model in CFD method is shown in Fig.12 and the comparison of the resistance in these conditions is represented in Tab.5.

(a) Test in the surface draft of 7 cm and speed of 1 m/s

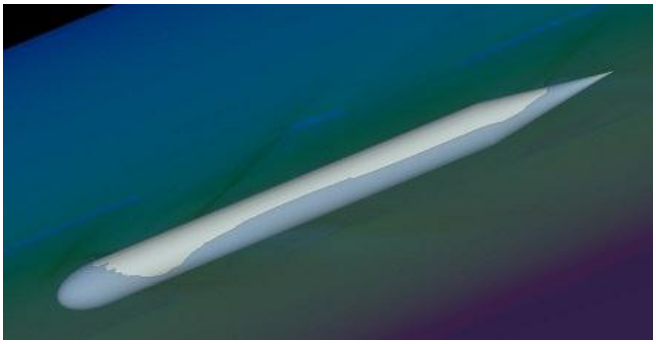

(b) CFD modeling in the same conditions of experiment

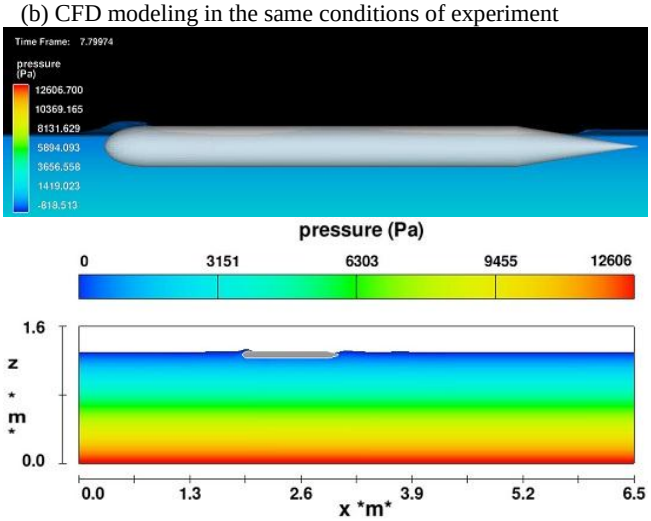

(c) General configuration of analysis in Flow-3D for the model

Figure 11: Comparison of the results of the experiment and CFD method (Flow-3D)

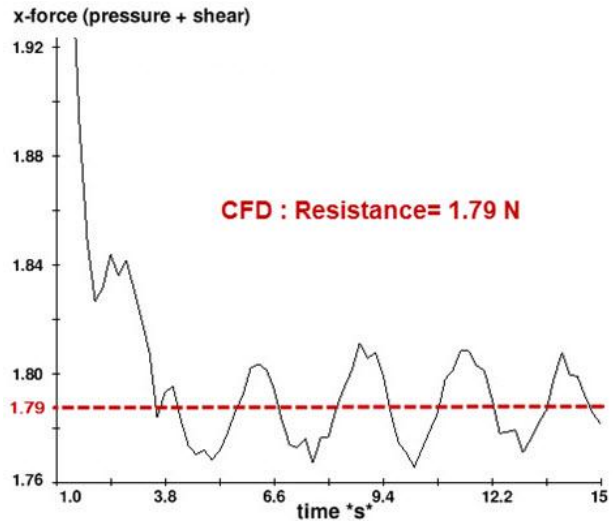

Figure 12. Total resistance in CFD method for case study validation

Table 5: Comparison of resistance

Resistance in experiment	1.67 (N)
Resistance in CFD	1.79 (N)
Difference	6.6 %

The difference of about 6.6 percentages is reasonable and acceptable. This validation case clearly shows the capability of a CFD tool, Flow-3D to reasonably predict the hydrodynamic problems of incompressible flow.

4-6- Results of CFD modeling

The results of CFD modeling for resistance are presented in Tab.6. Column 1 shows the resistance of submarine with strut (R_T) and column 2, shows the resistance only for strut (R_S) plus induced resistance (R_i) of strut. The column 3 is the difference of column 1 and 2 which should be equal to the resistance of body of submarine (R_B). It could be written as: $R_T=(R_S+R_i)+R_B$.

Induced resistance usually happens because of tip vortex effects of struts, which is an undesirable parameter and should be eliminated from the results. It meant that for achieving the net resistance of submarine hull, the induced resistance should be eliminated. As induced resistance is dependent on the struts, for a fair estimation, it can be stated as a percentage of the resistance of the strut. Column 4 shows the resistance of submarine without struts. Column 3 is smaller than column 4, because of existence of tip induced resistance of alone struts. When the struts stand on the body in experiment or CFD, the tip vortex would be eliminated. For solving the problem, by omitting the induced resistance in column 2, the values in column 3 will be increased and will be closer to values of column 4. As the result, the comparison of column 2 and 5 clarifies the role of induced resistance as approximately 70% of alone strut resistance (column 2)i.e: $R_i=0.7(R_S+Ri)$. Consequently, the modified results are applied on Tab.7. Application of this correction shows a good compatibility between column 3 and 4 in Tab.7.

Table 6. Initial CFD results of resistance

	(1)	(2)	(3)=(1)-(2)	(4)	(5)=(4)-(3)
V (m/s)	**R_T (N)**	**R_s+R_i (N)**	**Difference (N)**	**R_B (N)**	**R_i (N)**
0.2	0.20	0.02	0.18	0.22	0.04
0.3	0.30	0.04	0.27	0.29	0.02
0.39	0.41	0.11	0.29	0.38	0.09
0.49	0.54	0.18	0.37	0.50	0.13
0.60	0.75	0.26	0.49	0.70	0.21
0.71	0.98	0.34	0.64	0.90	0.26
0.80	1.27	0.45	0.82	1.19	0.37
0.9	1.61	0.55	1.06	1.44	0.38
1	2.10	0.68	1.42	1.95	0.53

Table 7. Modified CFD results of resistance

		(1)	(2)	(3)=(1)-(2)	(4)
	V (m/s)	Sub & Strut (N)	Modified Strut results (N)	Difference (N)	Submarine Only (N)
1	0.2	0.20	0.01	0.20	0.22
2	0.3	0.30	0.01	0.29	0.29
3	0.39	0.41	0.03	0.37	0.38
4	0.49	0.54	0.05	0.49	0.50
5	0.6	0.75	0.08	0.67	0.70
6	0.71	0.98	0.10	0.88	0.90
7	0.8	1.27	0.13	1.13	1.19
8	0.9	1.61	0.17	1.44	1.44
9	1	2.10	0.20	1.90	1.95

5- Discussion

Now the earned results of CFD modeling for the effect of induced resistance should be applied on the experimental results. Therefore, the induced resistance is eliminated by considering the 30% of initial values of strut resistance (Tab.8). The Comparison of the results of submarine bare hull resistance by CFD and experimental methods are presented in Fig.13. It shows some differences in low Froude numbers but a good adjustment in the usual range of Froude of submarines. In this range, the differences are between 7 to 9 percent. The reason of differences in low Froude numbers could be related to the laminar flow on the hull and absence of turbulator wire in CFD modeling. In experiments, there is a turbulator wire in the fore part of the body. For generalizing the results, resistance coefficients should be presented. These values are shown in Fig.14. In the usual Froude numbers (0.2~0.24) the resistance coefficient of bare hull of submarine with L/D= 13 (as usual in large submarines) at surface draft is in the range of 0.012~0.016 and in snorkel depth (depth equal to D) is in the range of 0.009~0.01.

Table 8. Modified experimental results

V (m/s)	Sub & Strut (N)	Strut (N)	Modified strut results (N)	Submarine Bare hull (N)
0.196	0.09	0.03	0.01	0.08
0.296	0.19	0.06	0.02	0.17
0.393	0.32	0.10	0.03	0.29
0.492	0.48	0.19	0.06	0.42
0.604	0.69	0.25	0.08	0.62
0.705	0.91	0.31	0.09	0.82
0.803	1.17	0.41	0.12	1.04
0.899	1.47	0.53	0.16	1.31
0.996	1.87	0.69	0.21	1.67

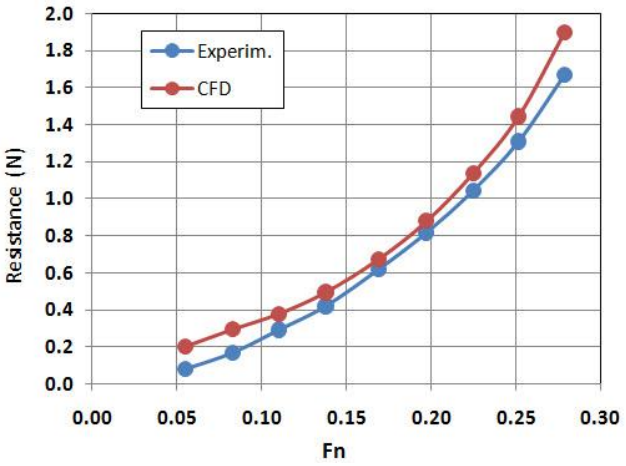

Figure 13. Comparison of the results of submarine bare hull resistance by CFD and experimental methods

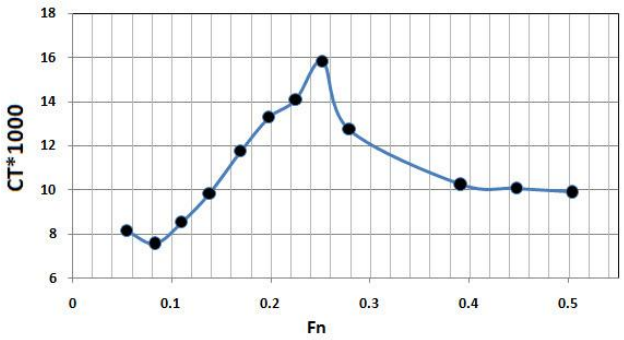

(a) at surface draft

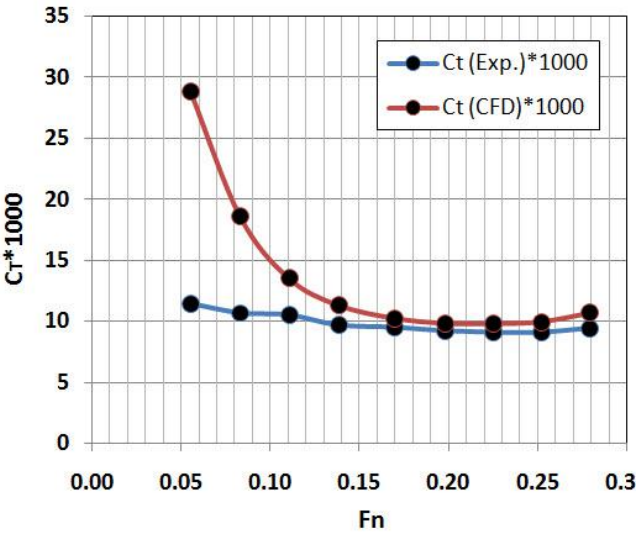

(b) at snorkel depth (=1D)

Figure 14. Resistance coefficients at surface draft and snorkel depth

6- Conclusion

This paper presented some technical notes for conducting the submarine model test in towing tank at near surface depth. Induced resistance between struts and hull is an important factor which should be evaluated exactly. This induced resistance could be considered 70% of resistance of alone struts with tip vortex effects. For a fair estimation, in the usual Froude numbers (0.2~0.24) the resistance coefficient at surface draft is in the range of 0.012~0.016 and in snorkel depth (depth equal to D) is in the range of

0.009~0.01. The cross section of struts for underwater test should be similar to water plan of ships. Foil shaped symmetric NACA shapes couldn't be a good advice because of large resistance and vibrations. Kapralon material has a good properties for the construction of submarine body for underwater tests.

Nomenclature

C_t	Total resistance coefficient based on wettedarea. $C_t=R_t/(0.5\rho AV^2)$
CFD	Computational Fluid Dynamics
D	maximum diameter of the outer hull [m]
DOF	Degree Of Freedom
Fn	Froude number - $Fn=V/\sqrt{g.L}$
GMO	General Mobile Object
h	depth from water level to the top of the submarine body [m]
H*	dimensionless depth (h/D)
IHSS	Iranian Hydrodynamic Series of Submarines
L	overall length of hull [m]
R_T	resistance of submarine with strut [N]
R_S	resistance only for strut [N]
R_B	resistance of body of submarine [N]
R_i	induced resistance [N]
V	model speed [m/s]

* Other parameters are shown on the figures or described inside the text.

7- References

1-Joubert, P.N., (2004),*Some aspects of submarine design: part 1: Hydrodynamics,*Australian Department of Defence.

2-Joubert, P.N., (2004),*Some aspects of submarine design: part 2: Shape of a Submarine 2026,*Australian Department of Defence.

3-Burcher, R. and Rydill, L.J., (1998),*Concept in submarine design,*The press syndicate of the University of Cambridge, Cambridge university press, p. 295.

4-Yuri, N.K. and Oleg, A.K., (2001),*Theory of Submarine Design,*Saint Petersburg State Maritime Technical University, Russia, pp.185-221.

5-Ulrich, G., (2000), *Submarine Design,* Bernard &GraefeVerlag.

6-Greiner, L., (1968),*Underwater missile propulsion* : a selection of authoritative technical and descriptive papers.

7-A group of authorities, (1990), *Submersible vehicle system design,* The society of naval architects and marine engineer.

8- Jackson,H.A., (1980), *Submarine Design Notes.*

9-Bertram, V.,(2000), *Practical Ship Hydrodynamics,* Elsevier Ltd., UK , pp. 369.

10-Rawson, K. J. and Tupper, E. C., (2001), *Basic Ship Theory,* Jordan Hill., Oxford, pp. 731.

11- Moonesun, M., Javadi, M., Charmdooz, P. and Korol, U.M., (2013),*Evaluation of submarine model test in towing tank and comparison with CFD and experimental formulas for fully submerged resistance,*Indian Journal of Geo-Marine Science, vol.42(8), p.1049-1056.

12-Moonesun, M., (2014),*Introduction of Iranian Hydrodynamic Series of Submarines (IHSS),*Journal of Taiwan Society of Naval Architects and Marine Engineers, Vol.33, No.3, p.155-162.

13- Rhee, K., Choi, J. and Lee, S., (2008), *Mathematical model of wave forces for the depth control of a submerged body near the free surface,* International offshore and polar engineering conference, Canada,

14- Polish,C.,Ranmuthugala,D.,Duffy,J. andRenilson,M., (2011), *Characterisation of near surface effects acting on an underwater vehicle within the vertical plane,* Australian Maritime College,.

15- Neulist, D., (2011), *Experimental Investigation into the Hydrodynamic Characteristics of a Submarine Operating Near the Free Surface,* Australian Maritime College, Launceston.

16- Dawson,E.,Anderson,B.,Steel,S.V.,Renilson,M. andRanmuthugala,D., (2011), *An experimental investigation into the effects of near surface operation on the wave making resistance of SSK type submarine,* Australian Maritime College,.

17-Haffenden, S. W.,(2009),*An Investigation into the Wave Making Resistance of a Submarine Travelling Below the Free Surfac,* Australian Maritime College, Launceston,.

18- Steel, S. V., (2010),*Investigation into the Effect of Wave Making on a Submarine Approaching the Free Surface,* Australian Maritime College, Launceston.

19-Moonesun,M. and Korol,Y.M., (2015), *Minimum Immersion Depth for EliminatingFree Surface Effect on Submerged Submarine Resistance,* Turkish Journal of Engineering, Science and Technology (TUJEST), vol.3, No.1, pp.36-46.

20- Moonesun, M., Korol, Y. and Dalayeli, H., (2015), *CFD Analysis on the Bare Hull Form of Submarines for Minimizing the Resistance*. 2 (3) :1-16 URL: http://www.ijmt.ir/browse.php?a_code=A-10-450-1&slc_lang=en&sid=1

21-Behzad,M.,Rad, M., Taghipour, R., Mousavi, S.M. andSadatHosseini, S.H., (2004), *Parametric study of hull operability in waves for a tourist submarine,* International Journal of Maritime Technology.

22-Hoerner, S.F., (1965),*Fluid Dynamic Drag,* USA.

23-Monesun, M., Korol, Y.M., Tahvildarzade,D. and Javadi,M. (2014), *Practical scaling method for underwater hydrodynamic model test of submarine*, Journal of the Korean Society of Marine Engineering, Vol. 38, No. 10 pp. 1217~1224, URL: https://sites.google.com/site/jkosme76/archives/back-issues.

24- Renilson, M., (2015), *Submarine Hydrodynamics,* Springer, pp.45-89.

Appendix A

2-1- Governing Equations

To solve the governing equations of fluid flow, Flow-3Duses a modification of the commonly used Reynolds-average Navier-Stokes (RANS) equations. The modifications include algorithms to track the free surface. The modified RANS equations are shown as:

$$\text{Continuity: } \frac{\partial}{\partial x}\left(uA_x\right)+\frac{\partial}{\partial y}\left(vA_y\right)+\frac{\partial}{\partial y}\left(wA_z\right)=0 \quad (1)$$

Momentum:

$$\frac{\partial U_i}{\partial t}+\frac{1}{V_F}\left(U_j A_j \frac{\partial U_i}{\partial x_j}\right)=\frac{1}{\rho}\frac{\partial P'}{\partial x_i}+g_i+f_i \quad (2)$$

The variables *u*, *v*, and *w* represent the velocities in the *x*-, *y*-, and *z*-directions; V_F = volume fraction of fluid in each cell; A_x, A_y, and A_z = fractional areas open to flow in the subscript directions; subscripts *i* and *j* represent flow directions;ρ = density; *P'* is defined as the pressure;U_j and $A_j$are velocity and cell face area in the subscript direction, respectively;g_i = gravitational force in the subscript direction; and f_i represents the Reynolds stresses for which a turbulence model is required for closure. It can be seen that, in cells completely full of fluid, V_F and A_j equal 1, thereby reducing the equations to the basic incompressible RANS equations.

2-2- Turbulences model

More recent turbulence models are based on Renormalization-Group (RNG) methods. This approach applies statistical methods for derivation of the averaged equations of turbulence quantities, such as turbulent kinetic energy and its dissipation rate. The empirically predicted coefficients of k-ε model are explicitly derived in RNG model. The transport equation of*k* is:

$$\frac{\partial k}{\partial t}+u\frac{\partial k}{\partial x}+v\frac{\partial k}{\partial y}+w\frac{\partial k}{\partial z}=P+G+D_k-\varepsilon \quad (3)$$

Where *k* is the turbulent kinetic energy, ε is the turbulent dissipation; *u*, *v* and *w* are velocities in *x*, *y* and *z* directions, respectively. *P* is the turbulence production term. P is computed using Eq. 4:

$$P=\frac{C_{SP}\mu}{\rho}\left[\begin{array}{l} 2\left(\frac{\partial u}{\partial x}\right)^2+2\left(\frac{\partial v}{\partial y}\right)^2+2\left(\frac{\partial w}{\partial z}\right)^2 \\ +\left(\frac{\partial v}{\partial x}+\frac{\partial u}{\partial y}\right)^2+\left(\frac{\partial u}{\partial z}+\frac{\partial w}{\partial x}\right)^2+\left(\frac{\partial v}{\partial z}+\frac{\partial w}{\partial y}\right)^2 \end{array}\right] \quad (4)$$

Where ρ is fluid density, μ is dynamic viscosity; C_{SP} is the shear production coefficient. In Eq. (3), G is the buoyancy production term:

$$G=\frac{C_\rho \mu}{\rho^3}\left[\frac{\partial \rho}{\partial x}\frac{\partial p}{\partial x}+\frac{\partial \rho}{\partial y}\frac{\partial p}{\partial y}+\frac{\partial \rho}{\partial z}\frac{\partial p}{\partial z}\right] \quad (5)$$

where C_ρ has a default value of 0.0 and in the case of buoyant flow, it would be 2.5. The diffusion term, D_k in Eq.(3) is:

$$D_k=\frac{\partial}{\partial x}\left(\frac{v_T}{\sigma_k}\frac{\partial k}{\partial x}\right)+\frac{\partial}{\partial y}\left(\frac{v_T}{\sigma_k}\frac{\partial k}{\partial y}\right)+\frac{\partial}{\partial z}\left(\frac{v_T}{\sigma_k}\frac{\partial k}{\partial z}\right) \quad (6)$$

Where v_T is turbulent viscosity σ_k = 1.0 in the standard $k-\varepsilon$ model and σ_k = 0.72 in the RNG $k-\varepsilon$model.The transport equation for ε is:

$$\frac{\partial \varepsilon}{\partial t}+u\frac{\partial \varepsilon}{\partial x}+v\frac{\partial \varepsilon}{\partial y}+w\frac{\partial \varepsilon}{\partial z}= C_{\varepsilon 1}\frac{\varepsilon}{k}\left(P+C_{\varepsilon 3}G\right)+D_\varepsilon-C_{\varepsilon 2}\frac{\varepsilon^2}{k} \quad (7)$$

where $C_{\varepsilon 1}$, $C_{\varepsilon 2}$ and $C_{\varepsilon 3}$ are user-adjustable non-dimensional parameters. The default value of $C_{\varepsilon 1}$ is 1.44 for the $k-\varepsilon$ model and 1.42 for the RNG.The default value of $C_{\varepsilon 2}$ is 1.92 for the $k-\varepsilon$ model but in the case of RNG model, it is computed based on the values of *k*, $\varepsilon$and the shear rate. $C_{\varepsilon 3}$ has the same value of 0.2 for both models. The diffusion term for the dissipation is:

$$D_\varepsilon=\frac{\partial}{\partial x}\left(\frac{v_T}{\sigma_\varepsilon}\frac{\partial \varepsilon}{\partial x}\right)+\frac{\partial}{\partial y}\left(\frac{v_T}{\sigma_\varepsilon}\frac{\partial \varepsilon}{\partial y}\right)+\frac{\partial}{\partial z}\left(\frac{v_T}{\sigma_\varepsilon}\frac{\partial \varepsilon}{\partial z}\right) \quad (8)$$

Where σ_ε = 1.3 in the standard $k-\varepsilon$ model and σ_ε = 0.72 in the RNG $k-\varepsilon$ model.

Generally, the RNG model is moreapplicablethan the standard k- ε model. In particular, the RNG model is more accurate in the case of low intensity turbulence flows and flows with strong shear regions. For simple flows, where the turbulence is in local equilibrium, the model provides results similar to the standard model.

2-3- Numerical methodology

The commercially available CFD package Flow-3D uses the finite-volume method to solve the RANS equations. The computational domain is subdivided using Cartesian coordinates into a grid of variable-sized hexahedral cells. For each cell, average values for the flow parameters (pressure and velocity) are computed at discrete times using a staggered grid technique (Versteeg and Malalasekera 1995). The staggered grid places all dependent variables at the center of each cell with the exception of the velocities u, v, and w and the fractional areas A_x, A_y, and A_z. Velocities and fractional areas are located at the center of cell faces (not cell centers) normal to their associated direction. For example, u and A_x are located at the center of the cell faces that are located in the Y, Z plane (normal to the X-axis). A two-equation renormalized group theory model, as

outlined by Yakhot and Orszag (1986) and Yakhotand Smith (1992), was used for turbulence closure. The modeling of a free-surface flow over an obstacle with Flow-3D constrains the makeup of each cell within the grid to one of five conditions: completely solid, part solid and fluid, completely fluid, part fluid, and completely empty. The problem was defined as an obstacle in the rectangular domain by the implementation of the Fractional Area/Volume Obstacle Representation (FAVOR) method. The free surface was computed using a modified volume-of-fluid (VOF) method.

2-4- Obstacle Generation

The FAVOR method, outlined by Hirt and Sicilian (1985) and Hirt (1992), is a porosity technique used to define obstacles. The grid porosity value is zero within obstacles and 1 for cells without the obstacle. Cells only partially filled with an obstacle have a value between zero and 1, based on the percent volume that is solid. The location of the interface in each cell is defined as a first-order approximation—a straight line in two dimensions and a plane in three dimensions, determined by the points where the obstacle intersects the cell faces. The slicing plane not only defines the fractional volume that can contain fluid but also determines the fraction area (A_x, A_y, and A_z) on each cell face through which flux (fluid flow) can occur.

It is obvious that smaller cell size will results in smoother obstacle boundary. It is important to note that, although short chords can effectively approximate a curved surface, it is still an approximation to a curved surface. To fit a curved surface exactly, a different numerical method such as a second order finite-element method or a curvilinear boundary fitted method would be required.

2-5- Free Surface Modeling

The accurate tracking offreesurface isvery important issue. Tracking involves three parts: locating the surface, defining the surface as a sharp interface between the fluid and air, and applying boundary conditions at the interface. One of the methods to track the free surface is the VOF method. The VOF method evolved from the marker-and-cell method (Harlow and Welsh 1965) but is more computationally efficient. The VOF method is described in Nichols and Hirt (1975), Nichols et al. (1980), and Hirt and Nichols (1981). Recently published work on the VOF method includes Kothe and Mjolsness (1992), Yamada and Takikawa (1999), and Colella et al. (1999). The VOF method is similar to the FAVOR method in defining cells that are empty, full, or partially filled with fluid. Cells without fluid have a value of zero. Full cells are assigned a value of 1 and partially filled cells have a value between zero and 1. The slope of the free surface within the partial cells is found by an algorithm that uses the surrounding cells to define a surface angle and a surface location. The VOF method allows for steep fluid slopes and breaking waves. Similar to the FAVOR method, the free surface is defined by a series of connected chords (2D) or by connected planes (3D); however, the VOF method allows for a changing free surface over time and space. Once again, this first-order approximation is not an exact fit to the curved flow surface. A true fit would require a second-order or higher adaptive grid that changes temporally and spatially to fit the changing water surface. The VOF method has additional concerns that require special consideration. VOF numerical techniques tend to be dissipative in nature, which can smear the free surface interface. Smearing of the interface distributes small amounts of fluid across several adjacent cells. These ‘‘misty’’ cells can introduce spurious results and prevent the free surface from being accurately identified. Flow-3D reduces this problem by implementing an algorithm to effectively clean up the misty regions (Flow-3D 1999). The implementation of this algorithm eliminates fluid in the misty regions and resets the fluid fraction in interface cells, thereby not completely adhering to the conservation of mass principle. The conservation of mass principle is additionally violated by computer round off error, as the code tracks fluid flux through cell face areas. However, the code also tracks the volume of fluid that is eliminated or added to the solution by the different algorithms. This cumulative volume error can provide a means of monitoring and evaluating the solution accuracy. In the final run of each numerical simulation, a cumulative volume error of less than 60.03% was reported.

Appendix B: Wave form in surface draft

V=0.2 m/s (Fn=0.05)

V=0.3 m/s (Fn=0.08)

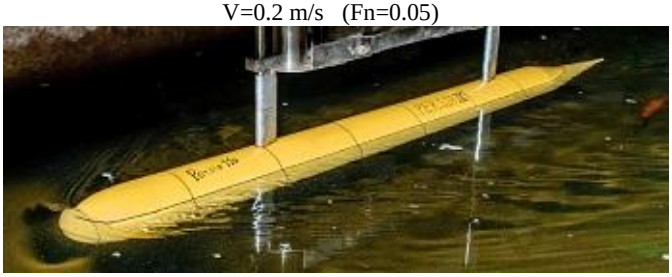

V=0.39 m/s (Fn=0.11)

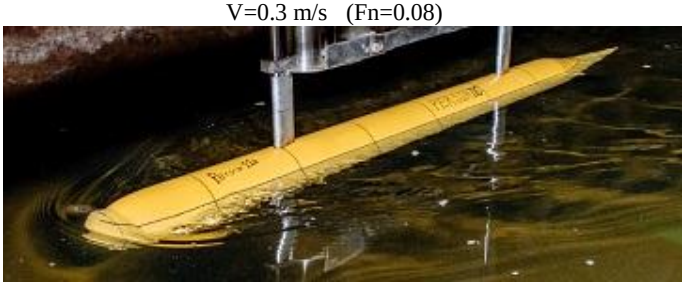

V= 0.49 (Fn=0.14)

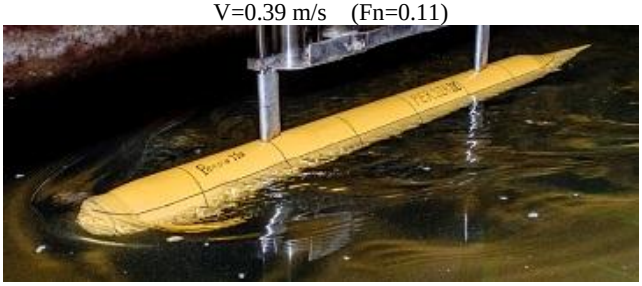

V= 0.6 m/s (Fn=0.17)

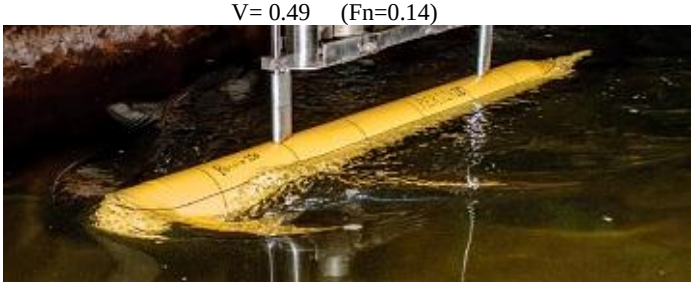

V= 0.7 m/s (Fn=0.2)

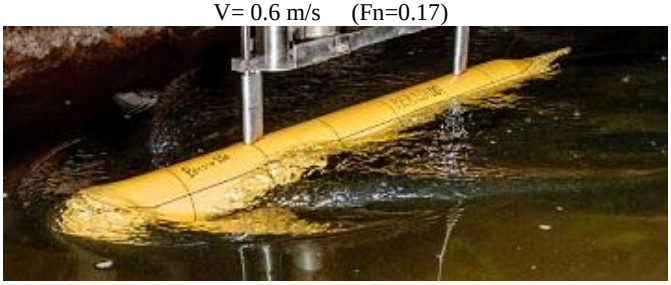

V= 0.8 m/s (Fn=0.22)

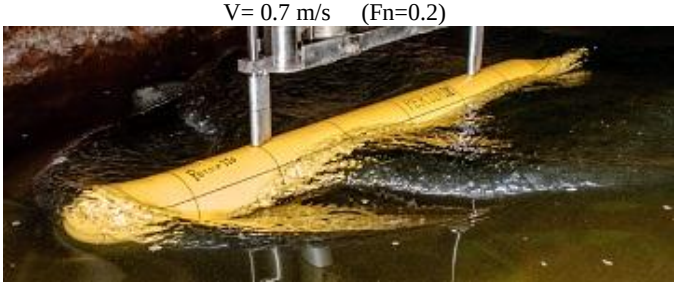

V= 0.9 m/s (Fn=0.25)

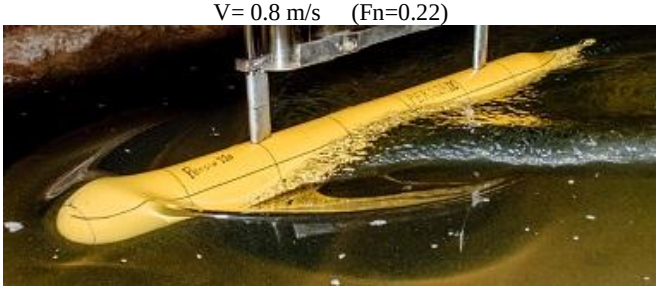

V= 1 m/s (Fn=0.28)

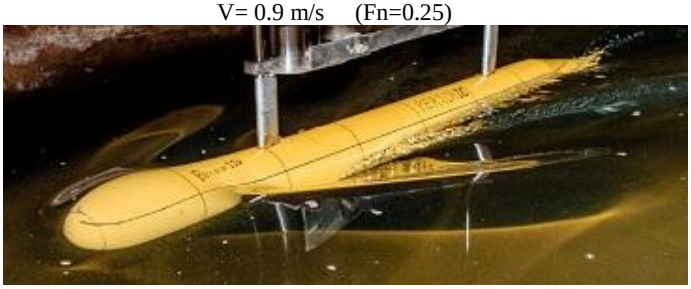

V= 1.4 m/s (Fn=0.39)

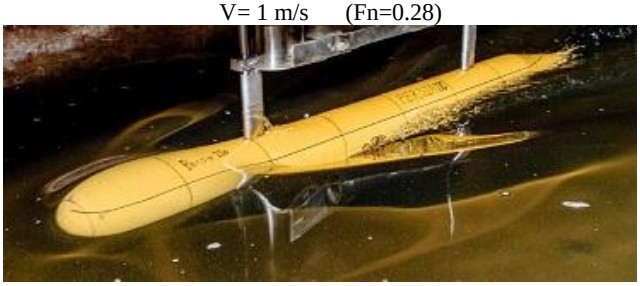

V= 1.6 m/s (Fn=0.45)

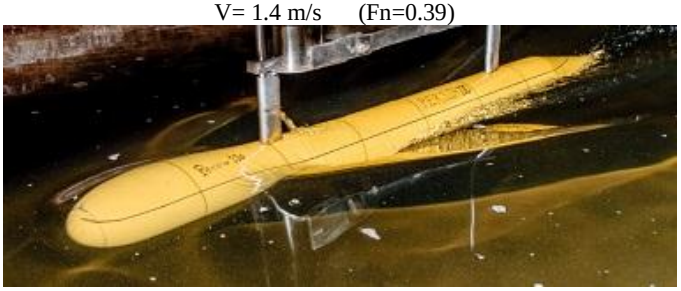

V= 1.8 m/s (Fn=0.5)

Appendix C: Wave form in snorkel draft: 100mm

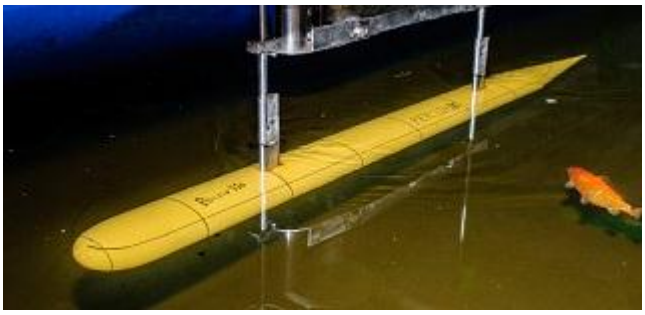

V=0.2 m/s (Fn=0.05)

V=0.3 m/s (Fn=0.08)

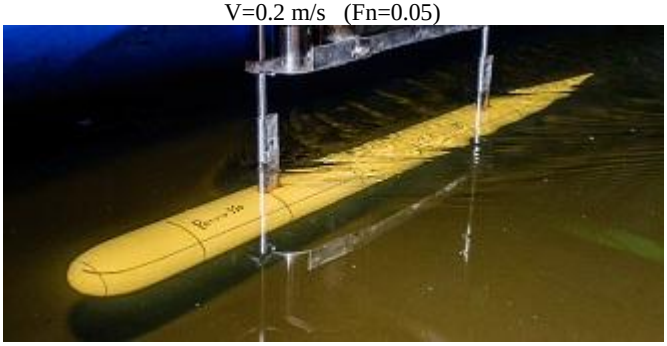

V=0.39 m/s (Fn=0.11)

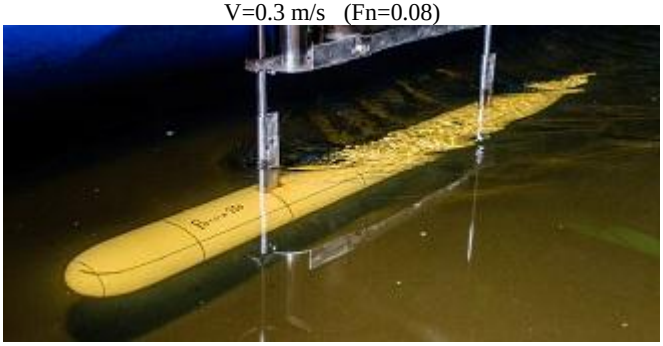

V= 0.49 (Fn=0.14)

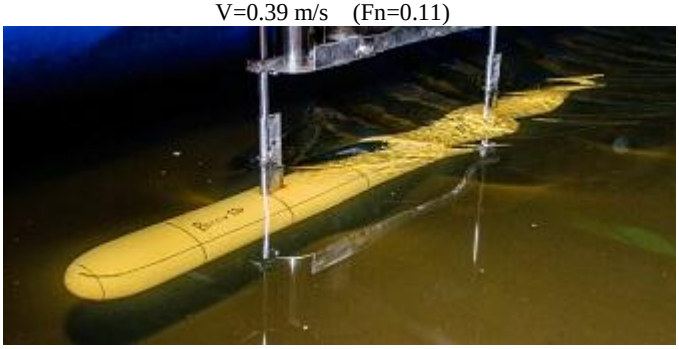

V= 0.6 m/s (Fn=0.17)

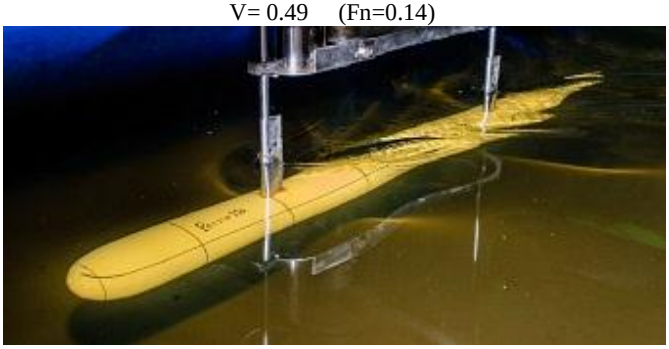

V= 0.7 m/s (Fn=0.2)

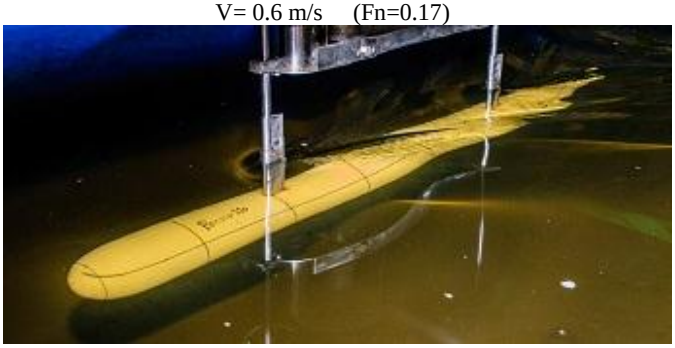

V= 0.8 m/s (Fn=0.22)

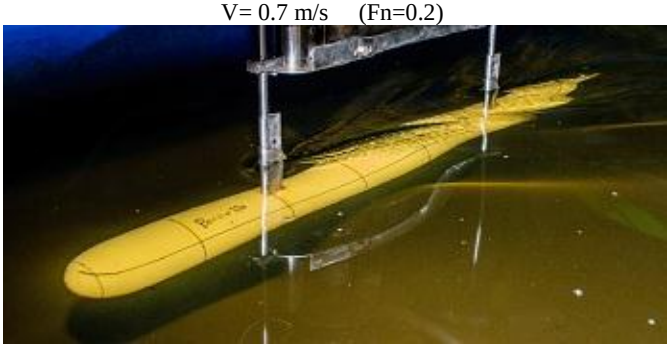

V= 0.9 m/s (Fn=0.25)

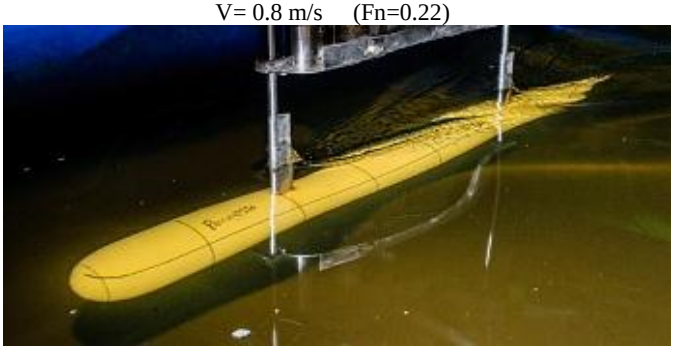

V= 1 m/s (Fn=0.28)

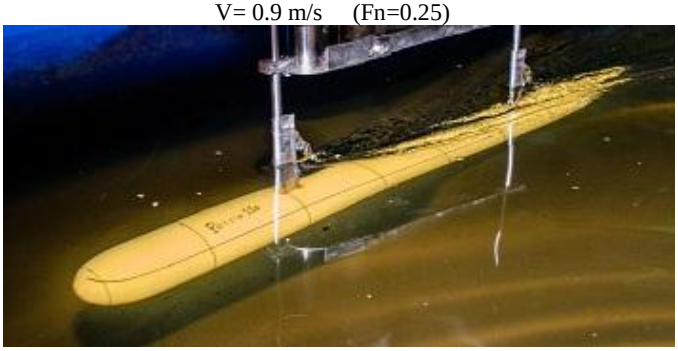

V= 1.4 m/s (Fn=0.39)

V= 1.6 m/s (Fn=0.45)

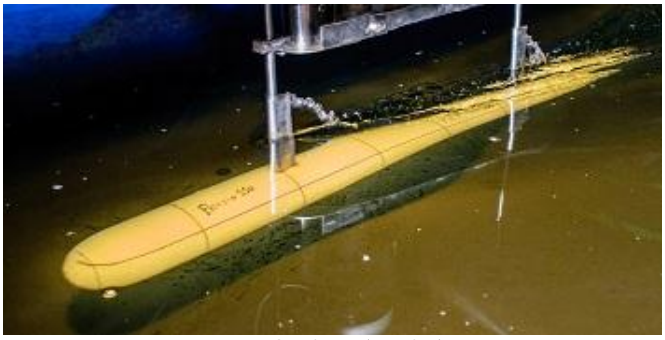

V= 1.8 m/s (Fn=0.5)

Appendix D: Wave form of strut at draft: 100mm

V=0.2 m/s

V=0.3 m/s

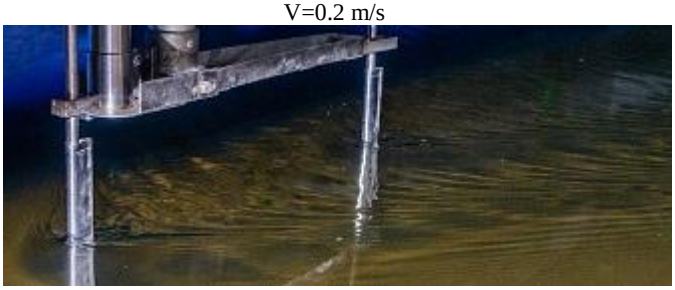

V=0.39 m/s

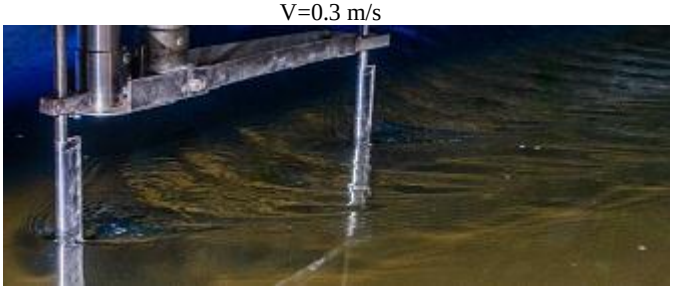

V= 0.49 m/s

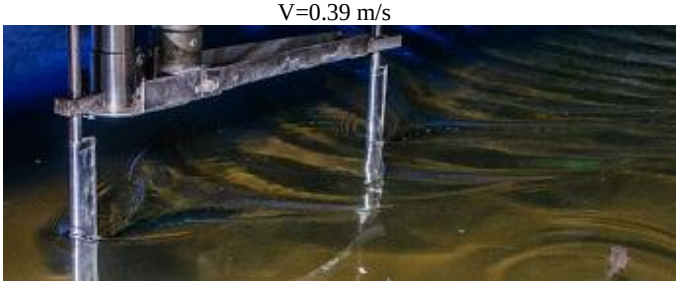

V= 0.6 m/s

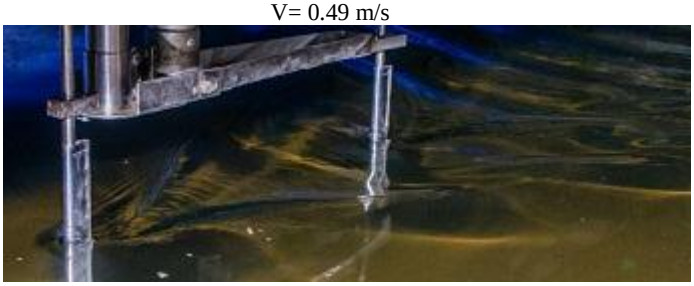

V= 0.7 m/s

V= 0.8 m/s

V= 0.9 m/s

V= 1 m/s